2014

Characterization of in-situ alloyed and additively manufactured titanium aluminides

Yan Ma
University of Wollongong, ym428@uowmail.edu.au

Dominic Cuiuri
University of Wollongong, dominic@uow.edu.au

Nicholas P. Hoye
University of Wollongong, nicholas.hoye@gmail.com

Huijun Li
University of Wollongong, huijun@uow.edu.au

Zengxi Pan
University of Wollongong, zengxi@uow.edu.au

Publication Details

Ma, Y., Cuiuri, D., Hoye, N., Li, H. & Pan, Z. (2014). Characterization of in-situ alloyed and additively manufactured titanium aluminides. Metallurgical and Materials Transactions B: Process Metallurgy and Materials Processing Science, 45 (6), 2299-2303.

Characterization of in-situ alloyed and additively manufactured titanium aluminides

Abstract
Titanium aluminide components were fabricated using in-situ alloying and layer additive manufacturing based on the gas tungsten arc welding process combined with separate wire feeding of titanium and aluminum elements. The new fabrication process promises significant time and cost saving in comparison to traditional methods. In the present study, issues such as processing parameters, microstructure, and properties are discussed. The results presented here demonstrate the potential to produce full density titanium aluminide components directly using the new technique. 2014 The Minerals, Metals & Materials Society and ASM International.

Disciplines
Engineering | Science and Technology Studies

Publication Details
Ma, Y., Cuiuri, D., Hoye, N., Li, H. & Pan, Z. (2014). Characterization of in-situ alloyed and additively manufactured titanium aluminides. Metallurgical and Materials Transactions B: Process Metallurgy and Materials Processing Science, 45 (6), 2299-2303.

Characterization of *In-Situ* Alloyed and Additively Manufactured Titanium Aluminides

YAN MA, DOMINIC CUIURI, NICHOLAS HOYE, HUIJUN LI, and ZENGXI PAN

Titanium aluminide components were fabricated using *in-situ* alloying and layer additive manufacturing based on the gas tungsten arc welding process combined with separate wire feeding of titanium and aluminum elements. The new fabrication process promises significant time and cost saving in comparison to traditional methods. In the present study, issues such as processing parameters, microstructure, and properties are discussed. The results presented here demonstrate the potential to produce full density titanium aluminide components directly using the new technique.

DOI: 10.1007/s11663-014-0144-6

I. INTRODUCTION

IT is generally recognized that gamma titanium aluminides are promising structural materials for high temperature aero engine and automotive applications, including turbine wheels, compressor blades, and pistons for reciprocating engines.[1–3] Central to such applications is the attractive combination of low density, unique mechanical properties, and resistance to oxidation.[4] Despite the desirable characteristics of γ-TiAl-based alloys, one of the major barriers to their widespread use has been associated with difficulties in processing and the subsequent high costs.[5]

Many improvements have been made in the production of γ-TiAl-based alloys using conventional casting, ingot forging, powder processing, and also new advanced techniques such as sheet production by hot-rolling, laser forming, and sintering. Although each of these processes is capable of producing material with acceptable properties, processing costs are still prohibitive for many commercial applications.[6,7] For conventional metals, additive layer manufacturing (ALM)[5,8] has been established as an economic alternative to conventional manufacturing methods such as casting and machining from billet. Additive layer manufacturing is used to produce complex, near net shape components through deposition of many consecutive layers in the form of powder or wire, offering high geometrical flexibility and major savings in time, material, and hence cost.[9] Significant effort has been devoted to developing ALM processes for alloys such as Ti-6Al-4V, while limited work has been done on intermetallics such as titanium aluminides. Murr *et al.*[10] and Biamino *et al.*[11] have recently succeeded in producing γ-TiAl-based alloy by powder-based additive manufacturing technology using electron beam melting (EBM) of γ-TiAl-based alloy powder, however, no information is available on the use of other heat sources or material feeding methods.

This paper evaluates the feasibility of producing γ-TiAl-based alloy components via additive layer manufacturing, using the gas tungsten arc welding (GTAW) process to deposit the intermetallic alloy *in-situ* from separate commercially pure titanium and aluminum wire feed stocks. Microstructural characterization and hardness properties of the as-fabricated alloy are presented.

II. EXPERIMENTAL METHOD

Several test "walls" measuring approximately 100 mm in length, 11 mm in height, and 10 mm in thickness were produced on a pure titanium substrate by multilayer deposition. A schematic drawing of the process is shown in Figure 1. The deposition process was protected from oxidation using an appropriately designed argon gas shielding device, but otherwise the process was performed out-of-chamber in open atmosphere. The feed materials were 1.0-mm diameter commercially pure titanium wire and 0.9-mm diameter pure aluminum welding wire. Wire feeding speeds of 700 mm/min for aluminum and 765 mm/min for titanium were selected in an effort to achieve a composition of Ti-44 at. pct Al. A welding current of 120 A was used at a travel speed of 95 mm/min.

The fabricated walls were sectioned into metallographic specimens, which were prepared using conventional metallographic procedures for titanium aluminides.[12] Optical micrographs were taken of the polished and etched cross-sections. The etching agent used was 6 vol. pct nitric acid and 3 vol. pct hydrofluoric acid in water. The microstructure and element distribution in the different regions of the specimens were analyzed by scanning electron microscopy (SEM, JEOL JSM-6490LA) equipped with an energy dispersive

YAN MA and NICHOLAS HOYE, Ph.D. Candidates, DOMINIC CUIURI and ZENGXI PAN, Senior Research Fellows, and HUIJUN LI, Associate Professor, are with the Faculty of Engineering and Information Sciences, University of Wollongong, Northfields Avenue, Wollongong, NSW 2522, Australia. Contact e-mail: ym428@uowmail.edu.au
Manuscript submitted December 20, 2013.

Published online: 05 August 2014

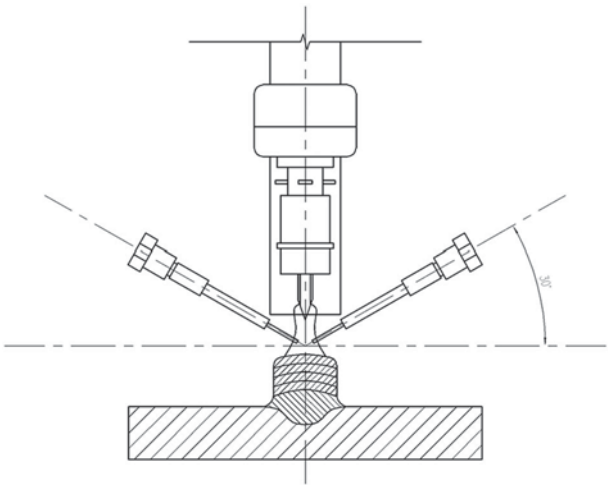

Fig. 1—Schematic drawing of the GTAW ALM process.

X-ray spectroscopy (EDS) analysis system. The accuracy of chemical composition measurements is ±1 at. pct. Phase identification was performed using a GBC MMA X-ray diffractometer (XRD) with CuKα radiation (λ = 1.5418 Å). Vickers microhardness profiles were measured on cross-sections of the specimens at a load of 200 g (HV0.2). In order to investigate a possible influence of location on hardness within the component, indentations were performed at the weld pool centre line from top to bottom in 0.5 mm intervals.

III. RESULTS AND DISCUSSION

A. *Microstructure and Composition*

The macro- and micro-structure of typical GTAW ALM-built wall specimen cross-sections are shown in Figures 2 and 3. The microstructure of titanium aluminides is typically characterized by γ-TiAl grains, a lamellar structure of $\gamma + \alpha_2$, or a combination of both.[13] Figure 2(a) displays the round top surface resulting from the surface tension of the molten material in the weld pool. Large elongated grains oriented parallel to the build-up direction (arrow) can also be observed, similar to those described in ALM-built Ti-6Al-4V products.[14] Nevertheless, the sequential welding layer bands documented in ALM of Ti-6Al-4V are not readily observed in the present samples. The process used in this study has many similarities to a multipass arc welding process. Solidification microstructures resulting from arc welding processes generally exhibit epitaxial growth from the adjacent melted substrate. The maximum driving force for solidification comes from the direction of the maximum temperature gradient, which is the direction perpendicular to the solid/liquid interface, and thus the preferential grain growth direction. Subsequent layers of grains continue to nucleate and grow from the previously coarsened grains. As the build-up continues, the unidirectional heat flow characteristic of the additive layer manufacturing process contributes to columnar grains growth.[15]

The delineation of top and bottom regions of the specimen is also displayed in Figure 2(a). Optical views of microstructure in the two regions are shown in Figures 2(b) (bottom region) and (c) (top region). SEM images exhibit higher magnification views in Figures 3(a) (bottom region) and (b) (top region). The sequential heating and cooling cycles produced by ALM create very specific microstructures revealing strong microsegregation within these two regions. The bottom region experiences periodic heat treatment by being subjected to temperature within the $\alpha_2 + \gamma$ phase field during consecutive GTAW ALM steps. This leads to the formation of a lamellar microstructure consisting of alternating platelets of γ and α_2 as seen in Figures 2(b) and 3(a), as well as interlocked grain boundaries. In contrast, the top region, which experiences the highest temperature in short time, displays long dendrites and white interdendritic phase, as shown in Figure 2(c). Similar conclusions have been drawn for titanium aluminide welds.[16,17] The higher magnification image (Figure 3(b)) reveals the interdendritic phase. In this area, deposition of the last ALM layer leads to heat treatment of the deposited materials above the α transus. According to the phase diagram,[18] peritectic reactions occur during solidification, however, they will hardly complete due to limited diffusion. Meanwhile, melt undercooling is expected to inhibit the formation of the pro-peritectic solid phase. The resulting enrichment of aluminum will occur in the remaining liquid progressively, which then solidifies as the interdendritic γ phase at lower temperature.[19]

Correspondingly, the chemical composition of different microstructure in different regions was identified by EDS analysis at the selected locations as shown in Figure 3, with results recorded in Table I. Lamellae in the bottom region have an average aluminum content of around 42.8 at. pct, while the interdendritic phase with higher aluminum content of around 45.0 at. pct is obtained in the top region. These measurements support the above hypothesis. In addition, the lamellar structures have similar chemical composition in different regions. It should be noted that the overall aluminum content is lower than that of expected from earlier calculations of the wire feed rates. The variation is not thought to be due to material loss during deposition. The process was very stable, produced neither spatter nor any visible fume indicative of high evaporative losses of aluminum. It is expected that the inconsistencies are due to variability of the wire feeding equipment under load, which can be corrected in future through improved control system design.

B. *Phase Identification*

In order to identify the phase structure, an XRD analysis of the GTAW ALM-built wall specimen was performed. XRD spectra obtained from the different regions are presented in Figure 4. Diffraction patterns in Figure 4(a) show the predominant peak in the bottom region is in the (201) plane corresponding to the α_2 phase located at $2\theta \approx 41$ deg. However, spectral peak heights indicate a γ/α_2 ratio ≈ 1 (52/48), suggesting similar

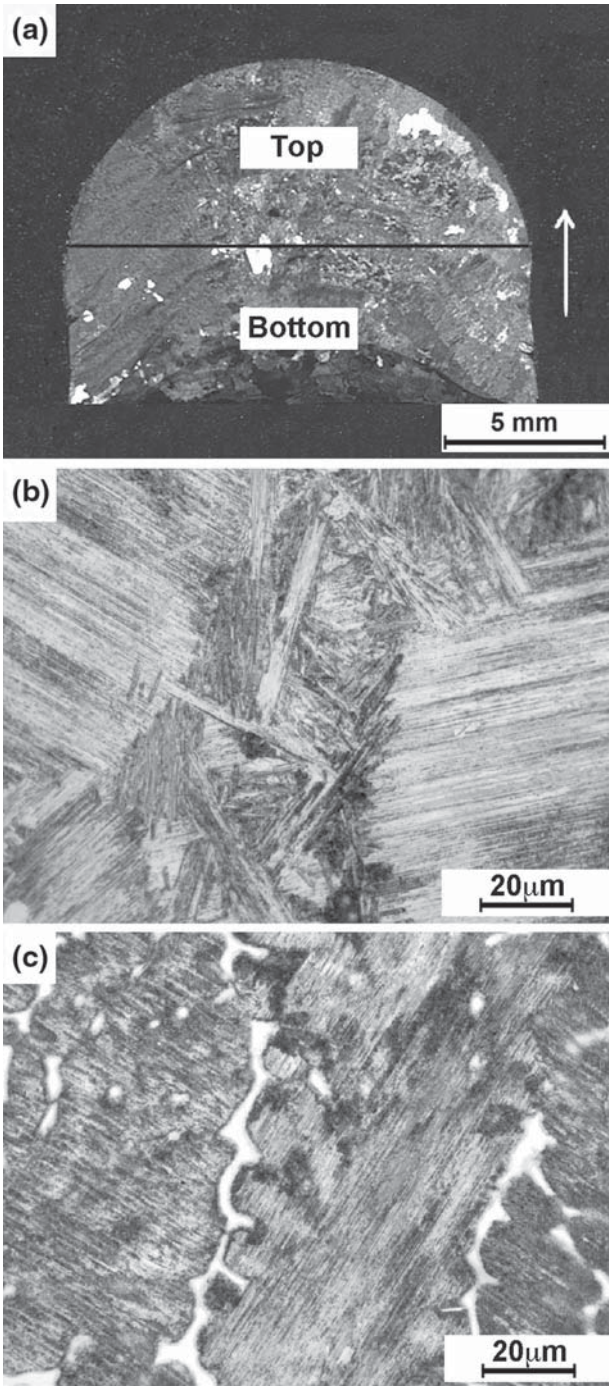

Fig. 2—Optical views showing morphology (*a*), microstructure in bottom region (*b*), and top region (*c*) on etched cross-sections of GTAW ALM-built wall specimen. In (a), different regions are identified, and the arrow shows the build direction.

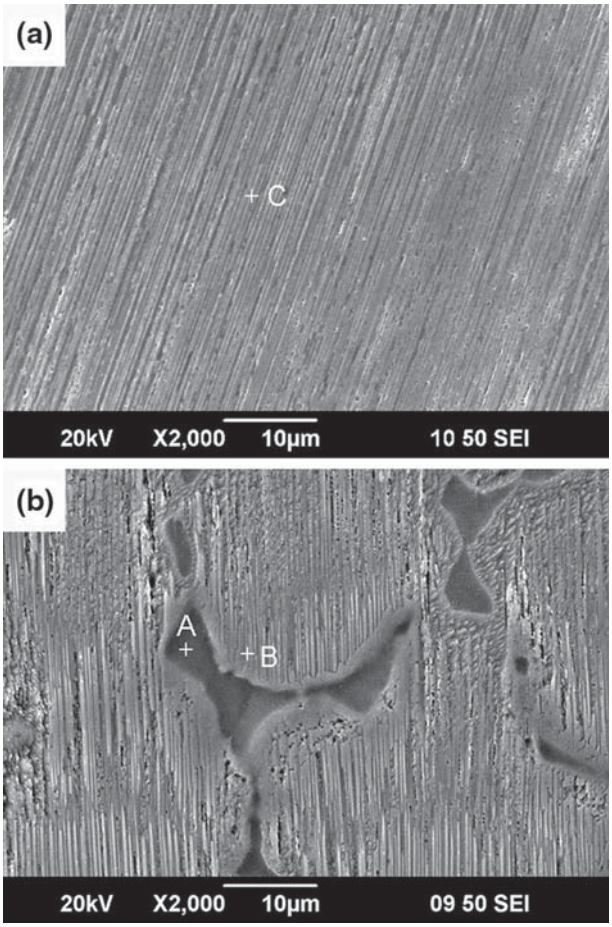

Fig. 3—SEM images showing representative microstructure in bottom region (*a*) and top region (*b*) on cross-sections of GTAW ALM-built wall specimen.

Table I. Chemical Composition of the As-Fabricated Materials, Determined by EDS

	Chemical Composition (At Percent)	
Location	Ti	Al
A	55.0	45.0
B	57.3	42.7
C	57.2	42.8

volume fractions of γ and α_2 phases. On the other hand, the top region (Figure 4(b)) exhibits a prominence of γ phase at approximately 39 deg with a ratio of $\gamma/\alpha_2 \approx 9$ (89/11), which includes both the γ lamellae and the interdendritic γ grains observed. There is a significant decrease in the α_2 phase in the top region compared to the bottom region. The weak intensity of the α_2 peaks could be attributed to the very thin α_2 lamellae. The volume fraction of different phases is controlled by the aluminum content and also strongly influenced by heat treatment and cooling rate[20] which is implicit in the GTAW ALM build process. This suggests that a high cooling rate linked to chilling by conduction into the substrate during initial weld passes plays an important role in the formation of α_2 phase in the bottom region.

C. *Hardness Analysis*

Microhardness (HV0.2) of the GTAW ALM-fabricated test specimen as a function of location is shown in Figure 5. Results illustrate that higher microhardness

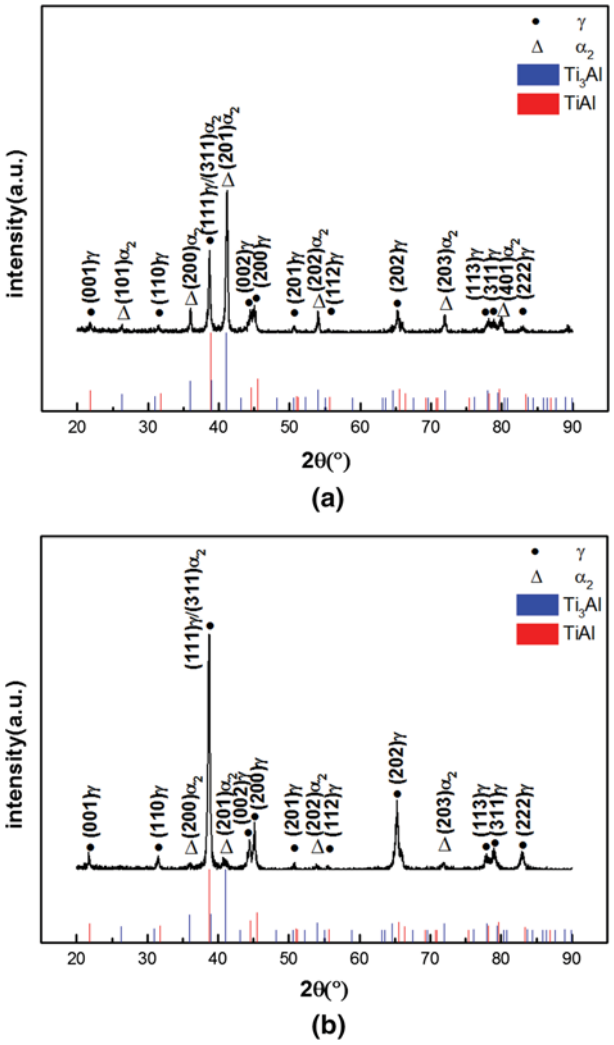

Fig. 4—XRD diffraction spectra for GTAW ALM-built wall specimen in different regions (*a*) bottom region (*b*) top region.

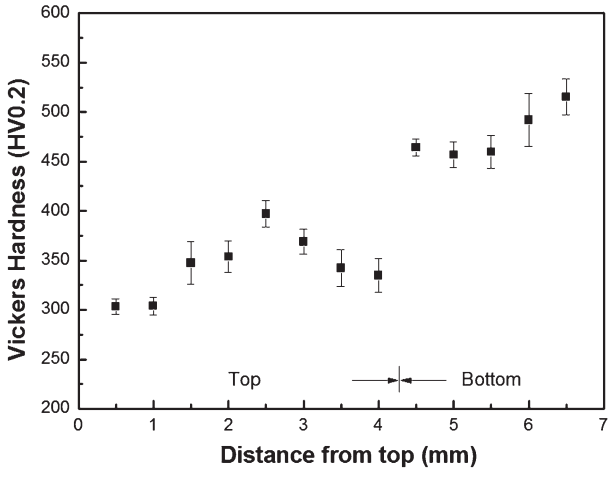

Fig. 5—Microhardness as a function of distance from the top of GTAW ALM-built wall specimen. Error bars show one standard deviation.

values are recorded in the bottom region with values decreasing toward the top. The α_2 phase is known to have a higher microhardness compared to other gamma-related phases.[21] As discussed earlier, it is believed that the different volume fractions of α_2 structures (Figure 4) in different regions results in the microhardness variation.

In addition, the top region has a maximum hardness value, which can be attributed to the inhomogeneous microstructure in this region. During the build-up process, the top region of the previous layer was partially re-melted every time a new layer was deposited on top of the existing layer. The materials underneath were heat-affected zones resulting from the sub-melting-point reheating treatment. After solidification, interdendritic γ phases surrounded by lamellar structure formed in the re-melted materials, while a fully lamellar structure was found in other regions. The indentation with maximum microhardness value in the top region was performed at thin lamellae in the reheated region, which are harder than thick lamellae or interdendritic γ phase.

IV. CONCLUSIONS

This preliminary study has investigated the feasibility of fabricating titanium aluminide components with *in-situ* alloying and additive layer manufacturing using the gas tungsten arc welding (GTAW) process with separate wire fed of the alloying elements. This process is able to successfully produce full density γ-TiAl-based alloy. The microstructure of as-fabricated materials presents strong microsegregation in different regions. The bottom region showed a lamellar (γ/α_2) structure and interlocked grain boundaries, whereas the top region revealed systematic occurrence of interdendritic γ phase. A microhardness gradient was observed over the height of the deposited wall. The relatively higher volume fractions of α_2 phase contributes to increased microhardness in the bottom region, and was due in part to the cooling characteristics of the GTAW ALM fabrication process.

ACKNOWLEDGMENTS

The authors gratefully acknowledge financial support from the China Scholarship Council (CSC), the University of Wollongong, and the Welding Technology Institute of Australia (WTIA).

REFERENCES

1. F. Appel, J.D.H. Paul, and M. Oehring: *Gamma Titanium Aluminide Alloys: Science and Technology*, 1st ed., Wiley-VCH, Germany, 2011, p. 729.
2. G. Sauthoff: *Intermetallics*, 2000, vol. 8, pp. 1101–09.
3. X.H. Wu: *Intermetallics*, 2006, vol. 14, pp. 1114–22.
4. H. Clemens and S. Mayer: *Adv. Eng. Mater.*, 2013, vol. 15, pp. 191–215.
5. D. Cormier, O. Harrysson, T. Mahale, and H. West: *Res. Lett. Mater. Sci.*, 2007, vol. 2007, pp. 1–4.

6. K. Kothari, R. Radhakrishnan, and N.M. Wereley: *Prog. Aerosp. Sci.*, 2012, vol. 55, pp. 1–16.
7. H. Clemens and H. Kestler: *Adv. Eng. Mater.*, 2000, vol. 2, pp. 551–70.
8. V. Petrovic, J.V. Haro Gonzalez, O. Jorda Ferrando, J. Delgado Gordilloa, J. Ramon Blasco Puchadesa, and L. Portoles Grinana: *Int. J. Prod. Res.*, 2011, vol. 49, pp. 1061–79.
9. F. Martina, J. Mehnen, S.W. Williams, P. Colegrove, and F. Wang: *J. Mater. Process. Technol.*, 2012, vol. 212, pp. 1377–86.
10. L.E. Murr, S.M. Gaytan, A. Ceylan, E. Martinez, J.L. Martinez, D.H. Hernandez, B.I. Machado, D.A. Ramirez, F. Medina, S. Collins, and R.B. Wicker: *Acta Mater.*, 2010, vol. 58, pp. 1887–94.
11. S. Biamino, A. Penna, U. Ackelid, S. Sabbadini, O. Tassa, P. Fino, M. Pavese, P. Gennaro, and C. Badini: *Intermetallics*, 2011, vol. 19, pp. 776–81.
12. V. Recina, J. Ahlström, and B. Karlsson: *Mater. Charact.*, 1997, vol. 38, pp. 287–300.
13. Y.W. Kim: *Acta Metall. Mater.*, 1992, vol. 40, pp. 1121–34.
14. B. Baufeld, E. Brandl, and O. Van der Biest: *J. Mater. Process. Technol.*, 2011, vol. 211, pp. 1146–58.
15. F. Wang, S. Williams, and M. Rush: *Int. J. Adv. Manuf. Technol.*, 2011, vol. 57, pp. 597–603.
16. G.Q. Wu and Z. Huang: *Mater. Sci. Eng. A*, 2003, vol. 345, pp. 286–92.
17. M.F. Arenas and V.L. Acoff: *Weld. J.*, 2003, vol. 5, pp. 110–15.
18. V. Raghavan: *J. Phase. Equilib. Diff.*, 2005, vol. 26, pp. 171–72.
19. D.M. Dimiduk: *Mater. Sci. Eng. A*, 1999, vol. 263, pp. 281–88.
20. B.W. Choi, Y.G. Deng, C. Mccullough, B. Paden, and R. Mehrabian: *Acta Metall. Mater.*, 1990, vol. 38, pp. 2225–43.
21. M.F. Arenas and V.L. Acoff: *Scripta Mater.*, 2002, vol. 46, pp. 241–46.